Development of Low Wind-Pressure Insulated Wires

*by Toshio Matsumura [*], Toshiki Yura [*], Naoshi Kikuchi [*2], Tetsuo Matsumoto [*3], Hitoshi Takeuchi [*4], Kunio Iwasaki [*5] and Yasuhiro Tominaga [*5]*

ABSTRACT Low wind-pressure insulated wires with a furrowed surface have been developed as a means to reduce the design load for electric poles and to suppress the reconstruction costs of electric poles at the time of restringing. It was demonstrated that the low wind-pressure wires not only enabled to reduce the wind load by more than 15 % compared to ordinary wires, but also were provided with excellent resistance against snow accretion. Moreover, in terms of basic performance such as electric characteristics, ease of stringing and adaptability for accessories, these wires were confirmed to be equivalent to ordinary wires.

1. INTRODUCTION

The design load for electric poles of power lines tends to increase due to the expanding electric power demands, causing the increase of facility costs. Because the design load greatly depends on the wind load on the strung wires, reduction of the wind load on the wires is expected to decrease the design load, thereby enabling to suppress the facility costs.

Until now, the study on wind pressure reduction has been focused on overhead transmission lines, in which several effective wire shapes have been found [1)~3)]. Thus wire shapes that are effective in reducing wind load have been investigated for wires 27 to 38 mm in diameter, while the study on overhead distribution lines using smaller wires 10 to 25 mm in diameter is still insufficient.

In this paper, wire shapes that are effective in reducing wind load have been studied with emphasis on insulated wires for overhead distribution lines using smaller wires, thereby achieving the development of practical insulated wires with low wind loads. Their characteristics will be reported in this paper.

2. INVESTIGATION ON WIRE CROSS SECTIONS

2.1 Mechanism of Wind Load Reduction

Mechanism of wind load reduction manifested by golf balls with a dimpled surface is well known, so that the same mechanism is applied to the wires to be developed at this time. Figure 1 shows the mechanism of wind load reduction on the wires. When the surface is furrowed, vortex is generated in the interior of the furrows. This reduces the shearing stress on the bottom of the boundary layer of airflow, mitigating the wind speed reduction at the boundary, and thus displacing the separation point to the leeward. This displacement decreases the number of vortex generated leeward reducing the pressure difference between the windward and the leeward of the wire, and eventually the wind load.

2.2 Wind Tunnel Experiment on Wire Models

2.2.1 Wire Models

In terms of overhead transmission lines, a wire shape with plural twisted grooves that are provided longitudinally on the wire surface is reported to be effective in reducing the wind load [1)]. This shape, however, is insufficient for wires with smaller diameters to achieve ample reduction of wind load with a design wind speed of 40 m/sec. Moreover, a special facility would be needed to form twisted grooves at extruding the insulated wires. Taking easy implementation of extrusion into consideration, various shapes of insulated wires for overhead distribution lines (e.g., 6-kV OC-I 80

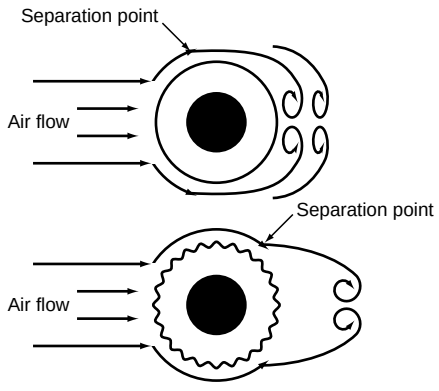

Figure 1 Mechanism of wind load reduction.

[*] Technical Research Center, The Kansai Electric Power Co., Inc.
[*2] Engineering Dept., Power Transmission Engineering Div.
[*3] Ecology and Energy Laboratory
[*4] Optical Components Dept., FITEL Products Div.
[*5] Engineering Dept., Power Cables Div.

mm², 15.6 mm in diameter) with a plurality of parallel furrows and ridges that are provided longitudinally on the wire surface were investigated in this study. We began by wind tunnel tests using wire models prepared by shaping an aluminum block in order to confirm the wire shapes that were effective in reducing wind loads.

Figure 2 shows cross sections of wire models used in the tests. The number of ridge was changed to study its effect on drag coefficients and, with 24-ridge and 30-ridge models, the height of the ridge was also changed to see the effects.

2.2.2 Method of Wind-Tunnel Test

Figure 3 shows the test equipment configuration. In the wind tunnel tests, a closed fuselage for measurement was installed at the air outlet, and a detector head for 3-component force measurement was used. Measured results were converted, according to the Reynold's number equation, to the wind speed for a wire diameter of 15.6 mm corresponding to 6-kV OC-I 80 mm², assuming an atmospheric condition of either 15°C, 1013 hPa or a typhoon in high-temperature seasons.

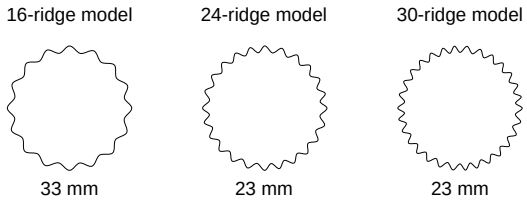

Figure 2 Cross sections of wire models for wind tunnel test.

2.2.3 Results of Wind-Tunnel Test on Wire Models

a) Effects of the number of ridge

Figure 4 shows the relationship between drag coefficient and wind speed for each wire model. The drag coefficient of every model is seen to have reduced compared to the ordinary wire at wind speeds of around 40 m/sec, decreasing in the order of 16-, 24- and 30-ridge.

The degree of the drag coefficient reduction is about 40 % for the 30-ridge model, a sufficient effect of reduction. A tendency can be seen that, as the number of ridge increases, both the wind speed at which the drag coefficient begins to drop and the wind speed at which the coefficient shows a minimum shift to the region of lower wind speed, and moreover, the minimum value of the drag coefficient decreases. From these results and in view of application to the wires of around 15 mm in diameter, it is

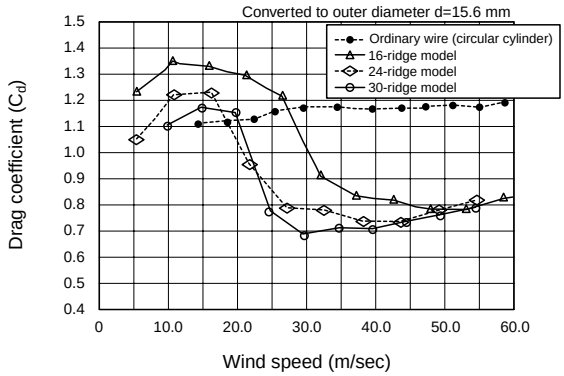

Figure 4 Relationship between drag coefficient and wind speed for wire models.

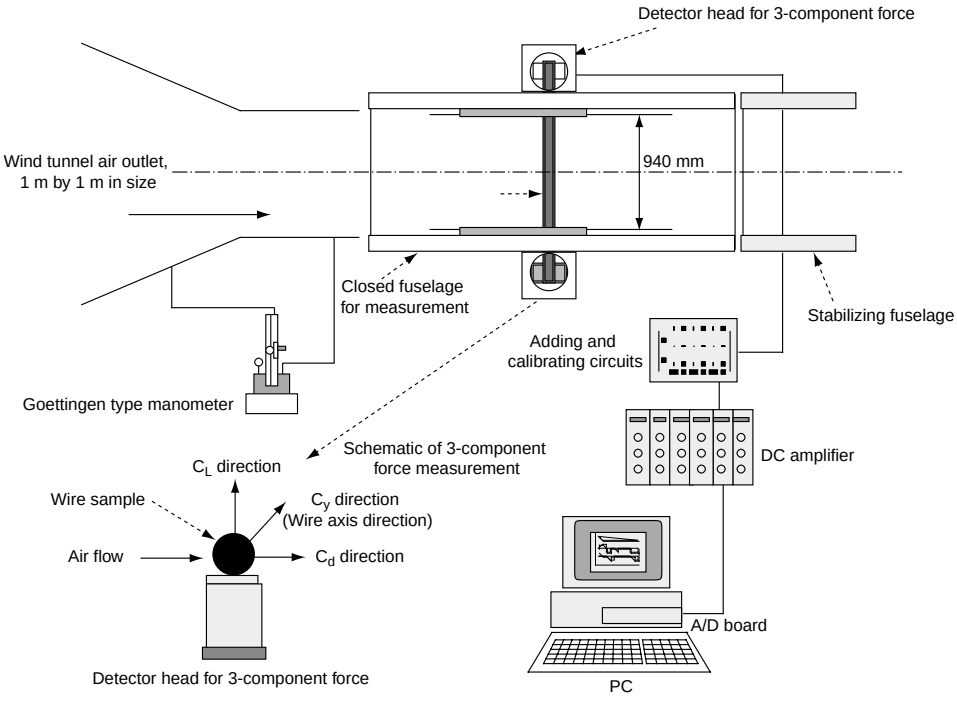

Figure 3 Equipment for wind tunnel test.

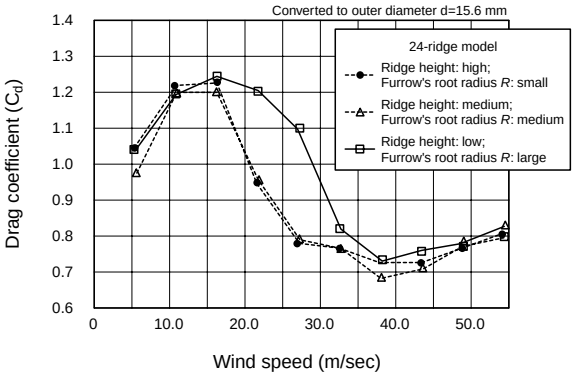

Figure 5 Effects of ridge height and furrow's root radius for 24-ridge model.

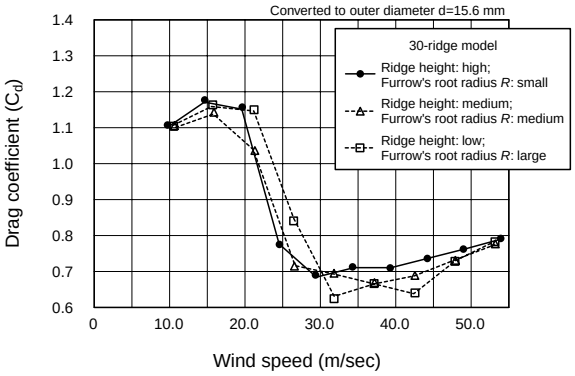

Figure 6 Effects of ridge height and furrow's root radius for 30-ridge model.

considered that the 30-ridge model represents the most suitable shape, which provides smaller drag coefficients at a wide range of wind speeds involving 40 m/s.

b) Effects of ridge height

Figures 5 and 6 show the relationships between drag coefficient and wind speed when the height of ridge and the furrow's root radius *R* are changed for 24-ridge model and 30-ridge model, respectively. The 24-ridge model shows small differences in the drag coefficient when the ridge height is medium or high, but when the ridge height is low, the wind speed at which the drag coefficient begins to decrease is seen to shift to the high wind speed range.

The 30-ridge model has been confirmed to show a relatively weak influence of ridge height on the drag coefficient. Thus, it is anticipated that the 30-ridge model achieves a stabilized effect of wind load reduction, when such practical issues as dimensional changes during insulation extrusion together with wire geometry changes due to dust accretion after stringing are taken into account.

c) Wind load reduction ratio on practical wires

In order to provide surface furrows on the insulation layer while ensuring an insulation thickness equivalent to ordinary wires, the outer diameter of the wire has to be larger than that of an ordinary wire. The wind load of each wire model has been calculated allowing for this diameter increase, in which it was assumed that the wire size to be OC-I 80 mm^2 and atmospheric conditions to be 23°C 960 hPa, a typhoon in high-temperature seasons. The results are shown in Figure 7. It has been confirmed that a sufficient wind load reduction can be expected regardless of increased diameter and that the 30-ridge model is most efficient in wind load reduction.

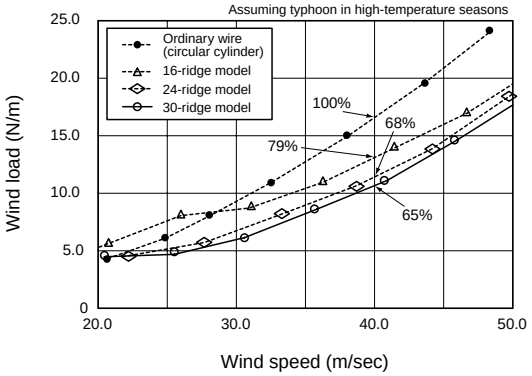

Figure 7 Calculated wind load on wire models, converted to OC-I 80 mm^2.

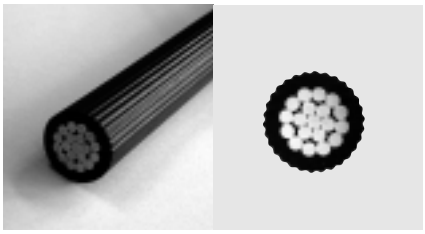

Photo 1 Low wind-pressure insulated wire, 6-kV OC 150 mm^2.

3. CHARACTERIZATION OF PROTOTYPE WIRES

3.1 Prototype Wires

It was demonstrated in the experiments based on aluminum models that the 30-ridge model achieved efficient wind load reduction, so that prototype wires of different sizes were fabricated using actual manufacturing facilities.

Photo 1 shows a low wind-pressure insulated wire, 6-kV OC 150 mm^2, thus fabricated. Using these prototype wires, wind load measurements at wind tunnel tests and that during rainfall were carried out, and their resistance against snow accretion was also evaluated.

3.2 Wind Tunnel Test

The equipment shown in Figure 3 were used in the wind tunnel tests of prototype wires. Rigidity of test samples was secured by a sample preparation process in which the insulation layer of a prototype wire was removed and subsequently reinstalled on a stainless steel shaft to make a sample.

Figures 8 and 9 show the wind speed vs. wind load relationship of 600-V OW-I 38 mm^2 and 22-kV OC-W 150 mm^2, respectively.

For all the cable sizes, the prototype of low wind-pres-

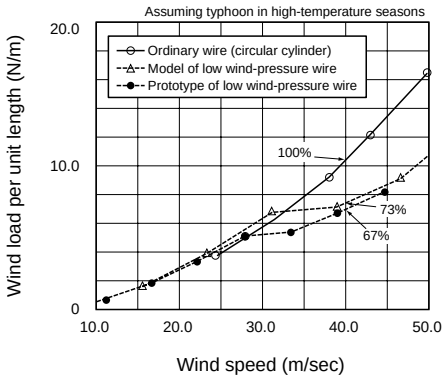

Figure 8 Relationship between wind load and wind speed on 600-V OW-I 38 mm² samples.

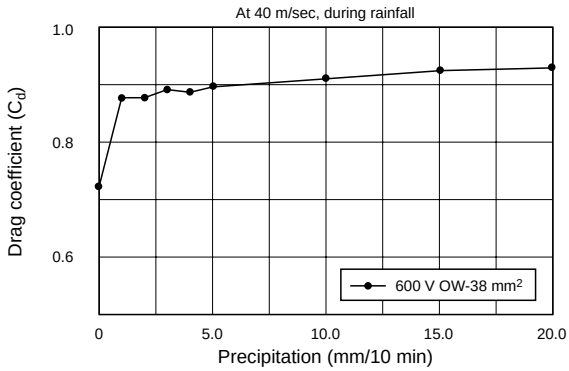

Figure 10 Relationship between precipitation and drag coefficient for 600-V OW-I 38 mm².

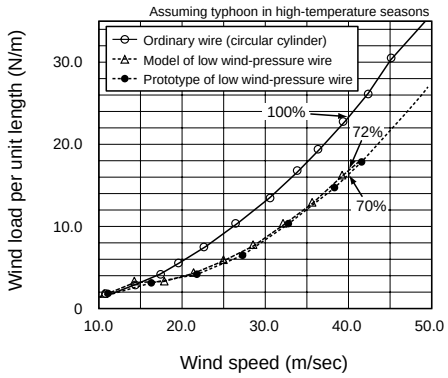

Figure 9 Relationship between wind load and wind speed on 22-kV OC-W 150 mm² samples.

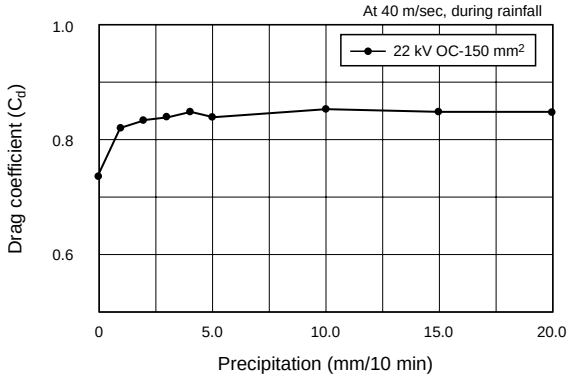

Figure 11 Relationship between precipitation and drag coefficient for 22-kV OC-W 150 mm².

sure wire shows a similar wind load changes as for the aluminum model, demonstrating that the surface condition and dimensional accuracy of wires actually fabricated were satisfactory in achieving an effect of wind load reduction that is equivalent to the shaped aluminum models. Thus the 30-ridge shape was validated to be sufficiently applicable to practical insulated wires.

Other wires of different sizes were also proved to provide the same level of wind load reduction as for the aluminum models.

3.3 Drag Coefficient Measurements during Rainfall

To clarify the effect of rainfall on the low wind-pressure wires, their drag coefficients were measured in which water drop spray was used to simulate rainfall. In the experiment, a pipe for water drop formation was installed on the windward of the measurement fuselage of wind tunnel test equipment shown in Figure 3, and drag coefficients at a wind speed of 40 m/sec were measured while a specified amount of water drop was sprayed simulating rainfall. Figures 10 and 11 show the precipitation vs. drag coefficient relationships of 600-V OW-I 38 mm² and 22-kV OC-W 150 mm², respectively.

The drag coefficient for either wire is seen to increase considerably at a light precipitation rate of about 1 mm/10min, and gradually increases as precipitation increases. The drag coefficient increase due to rainfall is larger for 600-V OW-I 38 mm² with a smaller outer diameter. The increase in drag coefficient due to rainfall may be attributable to a phenomenon such that raindrops adhere to the wire surface resulting in apparent changes in surface configurations, thereby suppressing the effect of wind load reduction.

In view of the 10-min precipitation data gathered at AMEDAS observation locations during 1994 to 1999, a precipitation rate of 15 mm/10min at a wind speed of 40 m/sec is sufficiently high, so that an evaluation test using a precipitation rate of 20 mm/10min would result in a suitable tolerance even when assuming typical typhoons.

Table 1 shows comparisons of wind loads at a wind speed of 40 m/sec with and without rainfall. It is seen that the prototype wires present, compared to ordinary wires, a wind load reduction of about 15 % at a precipitation rate of 20 mm/10min, while they present a wind load reduction of about 30 % under the condition of no precipitation.

3.4 Snow Accretion Resistance Test

Figure 12 shows equipment configuration for snow accretion resistance test. With this equipment, while a fan sends wind against wire samples, spray damping is used to moisten the snow that passes through a sieve thereby accelerating snow accretion. A video camera was used to monitor snow accretion, and the frequency with which the snow that had accreted on the sample fell down was

Table 1 Wind loads on prototype wires at a wind speed of 40 m/sec, represented in percentage over ordinary wires.

Voltage	Wire type	Wire size	Wind load under no precipitation (%)	Wind load under precipitation of 20 mm/10 min (%)
600 V	OW-I	38 mm^2	67	85
600 V	OW-I	60 mm^2	62	76
600 V	OW-I	100 mm^2	65	79
6 kV	OC	5 mm	Unmeasurable	Unmeasurable
6 kV	OC-I	80 mm^2	65	77
6 kV	OC-W	150 mm^2	62	73
22 kV	OC-W	150 mm^2	70	79

employed as a measure of snow accretion resistance.

Table 2 shows the results of evaluation of snow accretion resistance including those of a snow accretion resistant wire with fins. Snow accretion resistance was evaluated based on the fall times of accreted snow that took place during 10 minutes of snowfall and averaged over four experiments.

Whereas snow accreted on the surface of ordinary wire grew into a pipe-shaped snow, snow on both the low wind-pressure insulated wires and the snow accretion resistant wire with fins fell down immediately without growing. The low wind-pressure insulated wires are seen to have more fall times of snow compared to the snow accretion resistant wire with fins. Thus, the former wire compares favorably with the latter wire in terms of snow accretion resistance, and this result may be attributable to a mechanism such that the furrowed wire surface effectively suppresses the growth resulting from the rotation of accreted snow.

Furthermore, prototype wires were strung in an actual test field with a line span of 45 m to evaluate its snow accretion, in which it was confirmed that the low wind-pressure wires are superior to ordinary wires in snow accretion resistance.

3.5 Evaluation of Basic Characteristics as Electrical Wire

Various basic characteristics of prototype wires were evaluated in order to confirm that the change of the wire surface configuration did not have adverse influences on the basic characteristics of original electrical wires.

3.5.1 Evaluation of Electrical Characteristics

Electrical characteristics of all prototype wires were evaluated with respect to insulation resistance, AC withstand voltage, AC breakdown voltage and tracking resistance (for OC only), and it was confirmed that the wires were provided with electrical characteristics equivalent to those of ordinary wires.

3.5.2 Evaluation of Ease of Stringing

In order to evaluate the ease of stringing of prototype wires, 6-kV OC 150 mm^2 and 6-kV OC 80 mm^2 were evaluated for their adaptability to fittings and stringing tools including stripping jig, which was then followed by actual overhead stringing. As a result, it was confirmed that the wires were as easy to handle as ordinary wires.

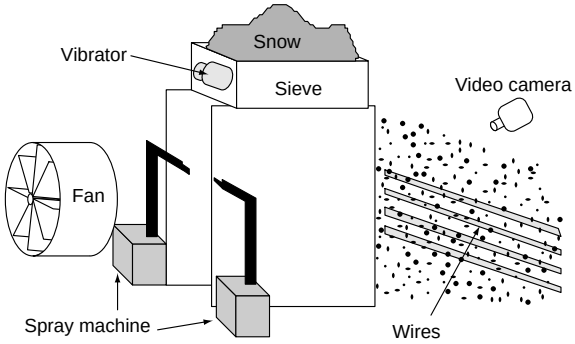

Figure 12 Equipment for snow accretion resistance test.

Table 2 Test results of snow accretion resistance of various wires.

	Voltage	Wire type	Size	Fall times of accreted snow in 10 min
Low wind-pressure insulated wire	6 kV	OC	5 mm	2.5 times
	6 kV	OC-I	80 mm^2	1.5 times
	6 kV	OC-W	150 mm^2	2.0 times
Snow accretion resistant wire with fins	6 kV	OC	60 mm^2	0.8 times
Ordinary wire	6 kV	OC	5 mm	No fall*

* Accreted snow on the ordinary wire did not fall but grew into a pipe-shaped snow.

3.5.3 Evaluation of Adaptability to Accessories

22-kV OC 150 mm^2, 6-kV OC 80 mm^2 and 5 mmϕ prototype wires were evaluated for their adaptability to overhead stringing accessories such as hot-melt joint cover and shrinking joint cover, whereby almost all of these accessories as they are now proved to be adaptable for use.

4. VERIFICATION FIELD TEST

A verification field test was carried out at Cape Shionomisaki in Wakayama Prefecture, using 6-kV OC 150 mm^2 and 6-kV OC 80 mm^2 prototype wires and ordinary wires.

Photo 2 shows the verification field test.

During the period from December 2000 to January 2001, winds perpendicular to the wires with a velocity of about 25 m/sec were observed. Figure 13 shows the relationships between wind speed and maximum tension of the 6-kV OC 150 mm^2 prototype wire and the ordinary wire, which were observed at a time instant close to the maximum wind speed. Effects of tension reduction due to the low wind-pressure shape can be identified to start at a wind speed of 18 to 20 m/sec and above, whereby a reduction of about 5 % in maximum tension has been

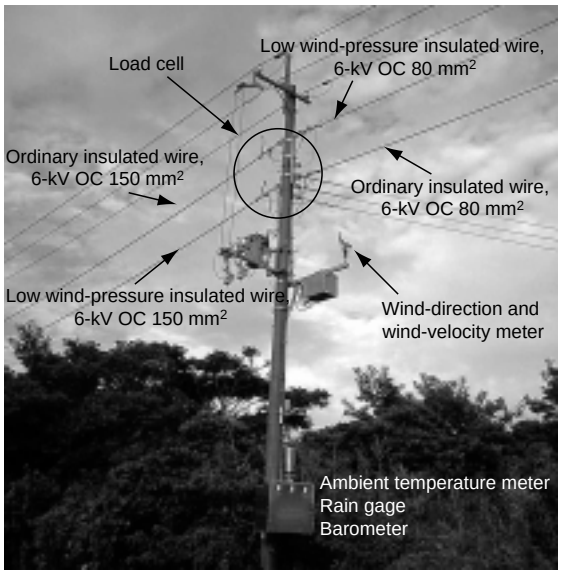

Photo 2 Verification field test at Cape Shionomisaki.

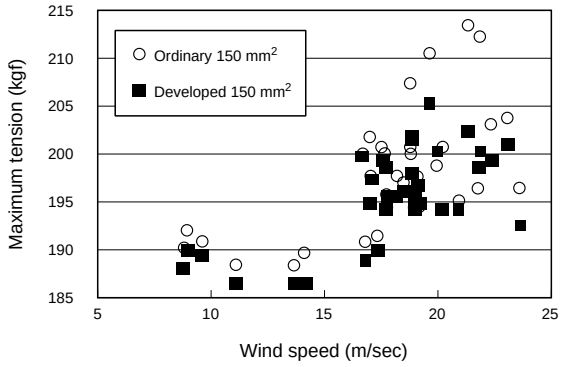

Figure 13 Relationships between wind speed and maximum tension of the developed and ordinary wires.

achieved.

Thus, the effectiveness of the prototype wires in wind load reduction has been demonstrated by the field test, while the wind speed range where the reduction effect appears approximately coincides with that encountered in the wind tunnel test.

5. SUMMARY

Various wire models with different surface furrows and ridges have been evaluated for their aerodynamic characteristics, and a superior wire shape applicable to insulated wires for overhead distribution lines has been found, which enables to efficiently reduce wind loads. Prototypes of these low wind-pressure insulated wires have been fabricated using actual manufacturing facilities, and have been subjected to evaluation experiments on their aerodynamic and snow accretion resistance characteristics. As a result, it was demonstrated that the wires not only reduced the wind load by more than 15 % compared to ordinary wires, but also provided excellent resistance against snow accretion. Selected wires of certain sizes were confirmed to be equivalent to ordinary wires in terms of basic performance such as electric characteristics, ease of stringing and adaptability to accessories.

REFERENCES

1) Ishikubo et al.: Study on wind load reduction of overhead transmission wires, Proc. IEEJ Energy Dept., p.580 (1995) (in Japanese)
2) Ishikubo et al.: Study on wind load reduction of overhead transmission wires: Part 3, Proc. IEEJ Energy Dept., p.753 (1996) (in Japanese)
3) Ishikubo et al.: Study on wind load reduction of overhead transmission wires: Part 3, Proc. IEEJ Electric Power and Energy Dept., p.776 (1997) (in Japanese)
4) Tsutahara et al.: Flow around a circular cylinder with arc grooves on its surface, Visualization Information, Vol.10, No.1, p.73 (1990) (in Japanese)
5) Eguchi et al.: Clarification on the mechanisms of wind load reduction on wires using fluidic experimentation, CRIEPI Report, U96050 (1997) (in Japanese)
6) IEEJ Survey Committee for Electric Standards, Design Standards for Structures for Electric Power Transmission, JEC-127-1979 (in Japanese)

Manuscript received on November 5, 2001.